

DEVELOPMENT AND OPTICAL ALIGNMENT OF EXPERIMENTAL MODEL FOR FORMOSAT-5 REMOTE SENSING INSTRUMENT

Po-Hsuan Huang^{*b}, Shenq-Tsong Chang^b, Yu-Cheng Cheng^a, Yu-Chuan Lin^a, Wei-Cheng Lin^b, Kuan-Huan Wu^a, Chia-Yen Chan^b, Ming-Ying Hsu^b, Po-Han Huang^a, Ho-Lin Tsay^b and Ting-Ming Huang^c

^aAssistant Researcher, Instrument Technology Research Center, National Applied Research Laboratories, 20, R&D Rd. VI, Hsinchu, 30076, Taiwan; Tel:+886-3-5779911#628;
E-mail: pohsuan@itrc.narl.org.tw

^bAssociate Researcher, Instrument Technology Research Center, National Applied Research Laboratories, 20, R&D Rd. VI, Hsinchu, 30076, Taiwan; Tel:+886-3-5779911#222;
E-mail: stc@itrc.narl.org.tw

^cResearcher, Instrument Technology Research Center, National Applied Research Laboratories, 20, R&D Rd. VI, Hsinchu, 30076, Taiwan; Tel:+886-3-5779911#229;
E-mail: tmw@itrc.narl.org.tw

KEY WORDS: Remote Sensing Instrument, Aerospace Telescope, Optical Alignment.

ABSTRACT: FORMOSAT-5 is a remote sensing satellite which is planned to be launched in 2014. Remote sensing instrument (RSI) with primary mirror diameter of 450 mm is the main payload on FORMOSAT-5. The remote sensing instrument experimental model (RSI ExM) is the preliminary model for verifying the alignment techniques and procedures of FORMOSAT-5 RSI.

The design, implementation and optical alignment of FORMOSAT-5 RSI ExM are introduced in this article. The design of RSI ExM follows the architecture of RSI baseline. Ritchey–Chrétien Cassegrain telescope with four element corrector lenses is adopted for the optical system design of RSI ExM, and the dimension is scaled down by the ratio of 0.622. Consequently, the effective focal length of RSI ExM is 2240 mm, and the diameter of primary mirror is 280 mm.

In order to verify the complicated alignment processes in advance, we establish a series of alignment procedures including alignment and bonding processes of primary mirror, alignment processes of coordinate measuring machine (CMM) aided primary and secondary mirror alignment, alignment processes of optical system alignment with interferometer and the measurement processes of system performance, etc. Moreover, we also design and establish highly precise auxiliary alignment fixtures (AAF) and mechanical ground support equipments (MGSE) to support all activities of RSI ExM assembly and alignment.

We have designed and fabricated all mechanical parts and optical lenses of RSI ExM in 2010. Now the optical system is processing the alignment processes and continues to improve alignment accuracy and system performance. All alignment processes of RSI ExM will be accomplished in the end of 2011 to meet FORMOSAT-5 RSI project schedule.

1. Introduction

In this paper, we will introduce the design, implementation and optical alignment of FORMOSAT-5 RSI ExM. FORMOSAT-5 is a remote sensing satellite which is planned to be launched in 2014. Remote sensing instrument (RSI) with primary mirror diameter of 450 mm is the main payload on FORMOSAT-5. In order to verify the alignment techniques and procedures of FORMOSAT-5 RSI, the remote sensing instrument experimental model (RSI ExM) has been kicked off in 2010 as a preliminary model for FORMOSAT-5 RSI. According to the purpose of RSI ExM, the design, structure, function and architecture will be simplified from RSI.

2. System Architecture

2.1 Optical Design

The design of RSI ExM follows the architecture of RSI baseline. Ritchey–Chrétien Cassegrain telescope with four element corrector lenses is adopted for the optical system design of RSI ExM, and the dimension is scaled down by the ratio of 0.622. Consequently, the effective focal length of RSI ExM is 2240 mm, and the diameter of primary mirror is 280 mm. Both the primary mirror and secondary mirror are hyperbolic surface with Schott Zerodur substrate. All four lenses of the corrector lens are spherical lens and their optical materials are FUSED SILICA. Figure 1(a)

shows the optical design of RSI ExM.

2.2 Structure Design and Opto-mechanical Design

The telescope structure of RSI ExM is truss structure with 6 carbon-fiber-reinforced polymer struts connecting with main plate and secondary mirror supporting ring, and the main plate is supported by two bi-pods on top panel, as shown in Figure 1(b). The 280 mm diameter primary mirror will be bonded with three iso-static mounts (ISM) by 3M DP490 structural adhesive and assembled on main plate. In the optical system design, we will fix primary mirror (M1) and adjust the orientation and position of the secondary mirror (M2) to align the optical system and meet the optical performance specification.

The secondary mirror will be bonded with adjustable supporting mechanism and supporting by M2 spider and M2 support ring. Most RSI ExM mechanical parts will be made by aluminum alloy Al7075T6, but the parts which will be bonded and assembled with optical materials were made by stainless steel SUS304, for the reason of coefficient of thermal expansion (CTE) match.

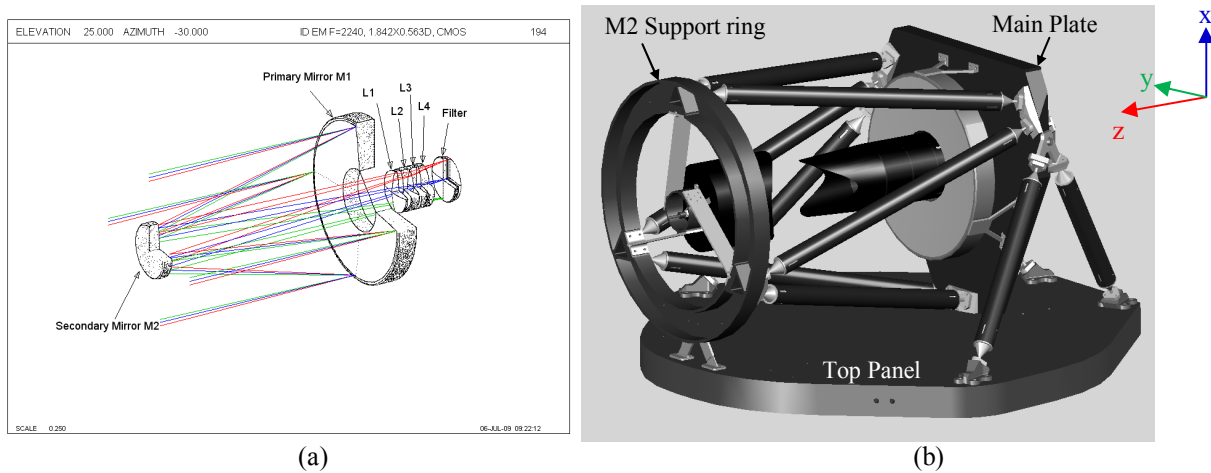


Figure 1. Optical system design of RSI ExM. (a) Optical design. (b) System architecture and coordinate system configuration.

In RSI ExM optical system, the secondary mirror adjustable supporting mechanism is a very important component for the telescope opto-mechanical system. In order to drive the optical performance of Cassegrain telescope optical system to approach diffraction limit, we must adjust the orientation and position of the secondary mirror very high precisely. Therefore, the adjustable supporting mechanism for secondary mirror shall be designed with five degrees of freedom for precise adjustment, and must be strong and robust enough to survive under the vibration condition which the G-force will be up to 25G during launch process.

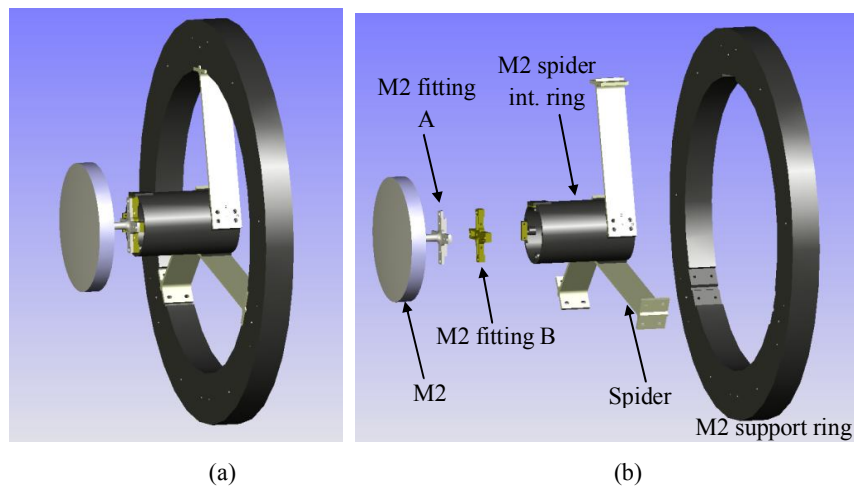


Figure 2. Secondary mirror supporting structures. (a) Secondary mirror assembly. (b) Exploded drawing and parts.

As Figure 3 shows, the secondary mirror (M2) will be assembled on supporting structure by M2 supporting assembly including M2 fitting A, M2 fitting B, M2 spider internal ring, spider and M2 support ring. Adjustable functions are designed and implemented in the following three mechanical parts: M2 fitting A, M2 fitting B and M2 spider internal ring. These parts will be assembled with very high re-position accuracy, and the minimum translation accuracy in X

and Y axis and minimum rotation accuracy about X and Y axis can reach $\pm 5 \mu\text{m}$ and ± 5 arcsecond, respectively.

3. Experiments and Verifications

3.1 Structural Adhesive Bonding Experiments and Vibration Test

In most aerospace applications, primary mirror will be mounted on structure by three iso-static mounts (ISM). Interfaces between primary mirror and ISMs are glued by structural adhesive. In order to study the bonding process and verify the bonding products, we established a series of experiments and verifications.

First, we fabricated a set of primary mirror and ISMs by transparent optical material PMMA for glue injection and bonding process study. As shown in Figure 3, the PMMA made primary mirror and ISMs were assembled on an auxiliary alignment fixture and supported by three precise stages. The bonding process would follow standard bonding procedure, including surface treatment, adhesive preparation, adhesive evacuation and adhesive curing. The 3M DP490 structural adhesive was injected into the space between ISMs and primary mirror, and the bond line was well controlled, as Figure 3(a) shows. According to the primary mirror and ISMs were transparent, we could observe the adhesive flow during injecting process and inspect the injection result which if the adhesive could fill up the whole chamber between ISM and primary mirror, as Figure 3(b) shows.

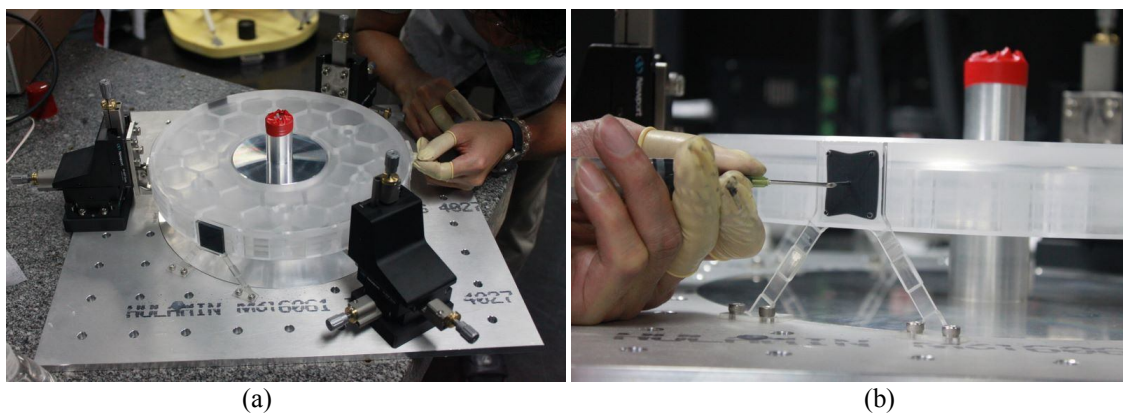


Figure 3. Structural adhesive bonding experiments for transparent ISMs and primary mirror.

After the study of bonding process, we bonded and assembled two sets of dummy primary assembly for vibration test to verify the bonding strength and structure strength of the M1-ISMs assembly. In this experiment, the dummy primary mirrors and main plate were made by aluminum alloy Al6061 with lightweighting structure, and the ISMs were made by stainless steel SUS304.

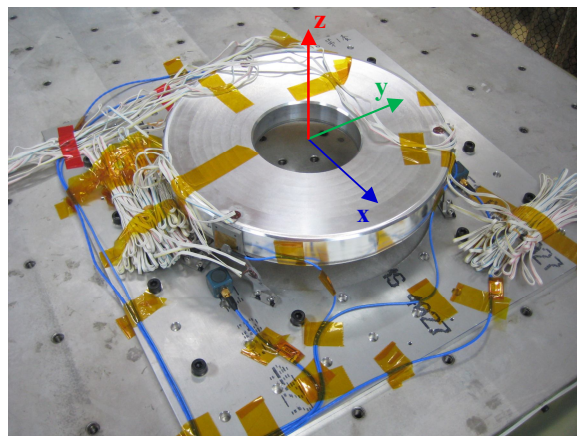


Figure 4. Vibration test set up of the M1-ISMs assembly on vibration test platform and coordinate configuration.

As Figure 4 shows, during vibration test, M1-ISMs assembly were set up on vibration test platform and fixed by several M10 screws. Three controlled accelerometers and three measured accelerometers were attached on the assembly for vibration control and measurement. The vibration test conditions are shown in Table 1, in each direction, there are four test sequences: pre-low sine sweep, mediated vibration, full vibration and post-low sine sweep. The maximum G-force will be up to 25.0 G in X direction. By visual and ultrasonic inspection, and comparing the measured frequency response between post-low sine sweep and pre-low sine sweep, we can determine if the assembly structure were damage by vibration test. Finally, both dummy M1-ISMs assembly passed vibration test without any damage.

Table 1. Vibration test conditions for M1-ISMs assembly

Se.		X	Y	Z
1	Pre-low sine sweep	0.2G, 5-500 Hz, 2 Oct/min	0.2G, 5-500 Hz, 2 Oct/min	0.2G, 5-500 Hz, 2 Oct/min
2	Mediated	12.5G, 20-24 Hz, 1 Oct/min	7.5G, 20-24 Hz, 1 Oct/min	7.5G, 20-24 Hz, 1 Oct/min
3	Full	25.0G, 20-24 Hz, 1 Oct/min	15.0G, 20-24 Hz, 1 Oct/min	15.0G, 20-24 Hz, 1 Oct/min
4	Post-low sine sweep	0.2G, 5-500 Hz, 2 Oct/min	0.2G, 5-500 Hz, 2 Oct/min	0.2G, 5-500 Hz, 2 Oct/min

3.2 Verification for Re-position Accuracy and Repeatability of Secondary Mirror Adjustable Supporting Mechanism

After design concept development and detail mechanical design were accomplished, the performance of proposed secondary mirror adjustable supporting mechanism has to be verified by experiments. Figure 5 shows the experiment setup. M2 spider internal ring has been modified to fix on the granite table by two M8 stainless steel screws. A flat mirror with Pyrex substrate and 5 cm diameter, which flatness is better than $1/8 \lambda$, has been bonded with M2 fitting A by 3M DP490 structural adhesive. M2 fitting A, M2 fitting B, decenter shims and experimental base were fabricated by stainless steel SUS304 and SUS402, and M2 spider internal ring is manufactured by aluminum alloy Al7075T6.

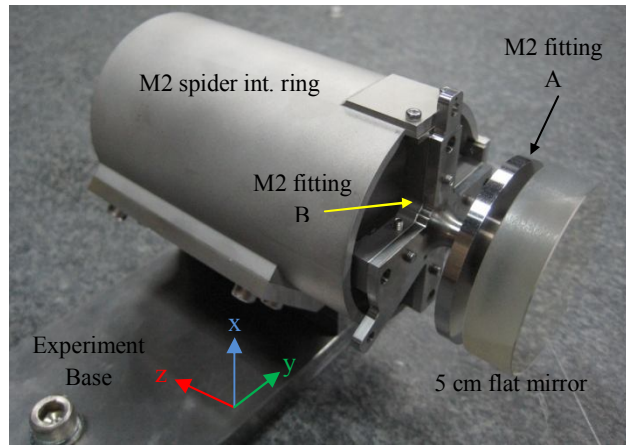


Figure 5. Experiment setup for adjustable supporting mechanism verification.

The first verification will check the re-position accuracy and tilt repeatability. We released and reassembled the assembly and use the Leica TM5100A theodolite to measure the angle variation of the 5 cm flat mirror. Figure 6(a) shows that tilt variations of M2 fitting A versus M2 fitting B are less than 5 arcsecond, and the average is 2.94 arcsecond. Figure 6(b) shows that tilt variations of M2 fitting A & B assembly versus M2 fitting internal ring are less than 10 arcsecond, and the average is 5.01 arcsecond.

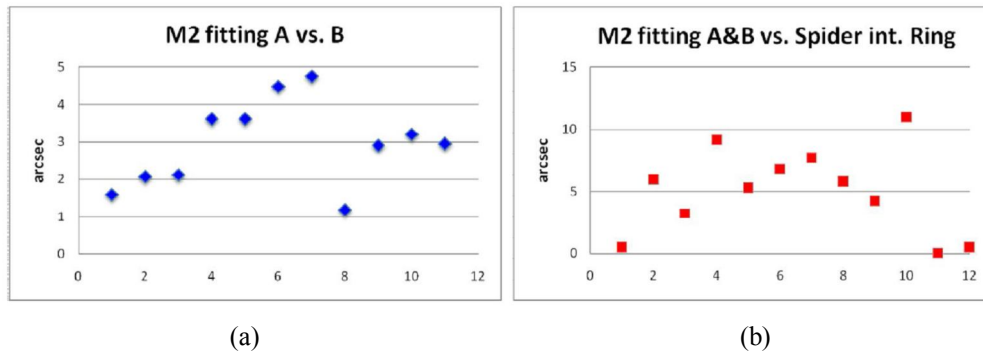


Figure 6. Experimental results of re-position accuracy and tilt repeatability.

The re-position accuracy and decenter repeatability were also verified. We released and reassembled the assembly repeatedly with 18 times and used the coordinate measuring machine (CMM) to measure the position of the 5cm flat mirror. This experiment also was divided into two parts, the first one verified the re-position accuracy of M2 fitting A versus M2 fitting B, second part verified the re-position accuracy of M2 fitting A & B assembly versus M2 spider internal ring.

In this experiment, we used the Brown & Sharpe Global Image 9128 coordinate measuring machine (CMM) to measure the position of mirror surface of 5 cm flat mirror, and detected the position of mechanical axis of the 5 cm

ringed mirror. By analyzing these data, we could obtain the information of re-position accuracy and decenter repeatability of the assembly.

Figure 7 shows the verification results. The measured position variations of M2 fitting A versus M2 fitting B all are less than $\pm 1 \mu\text{m}$ in three directions (Figure 7(a)). Another test result is shown in Figure 7(b). The measured position variations of M2 fitting A & B assembly versus M2 fitting internal ring are less than $\pm 5 \mu\text{m}$ in three directions. In this case, the re-position accuracy in Z axis is obviously better than that in other two axes, and the standard deviation for 18 measurements is $1.66 \mu\text{m}$.

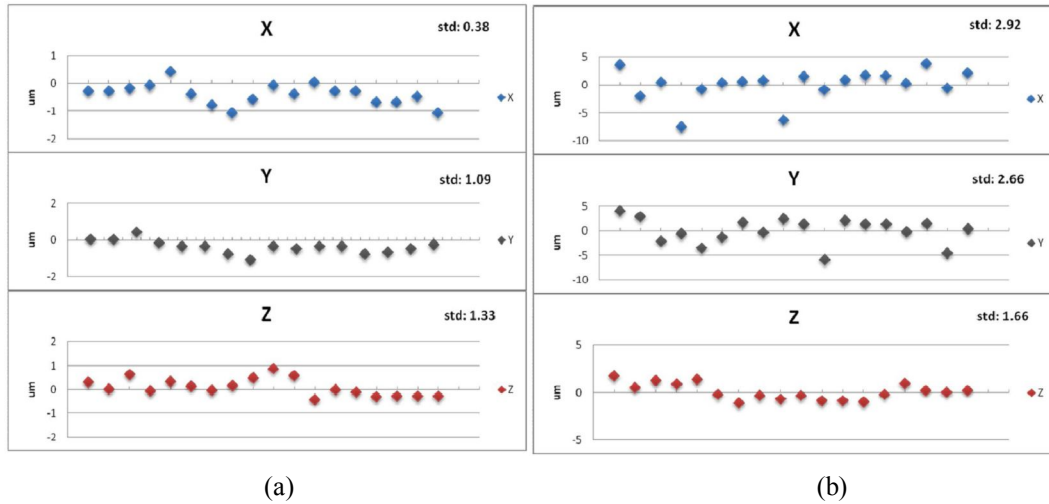


Figure 7. (a) Re-position accuracy of M2 fitting A versus M2 fitting B. (b) Re-position accuracy of M2 fitting A & B assembly versus M2 fitting internal ring.

4. Optical Alignment

4.1 Primary Mirror Bonding and Alignment

According to alignment procedure, the primary mirror will be aligned first. As Figure 8 shows, this process was implemented on an auxiliary alignment fixture and the primary mirror is supported by three stages which minimum adjustment accuracy is $1 \mu\text{m}$. We used coordinate measuring machine to measure the surface of primary mirror and the mechanical axis of main plate respectively. After that, we adjusted the stages to align the optical axis with mechanical axis according to calculated results from measured data. Finally, the aligned result was 10.2 arcsecond between the two axes.

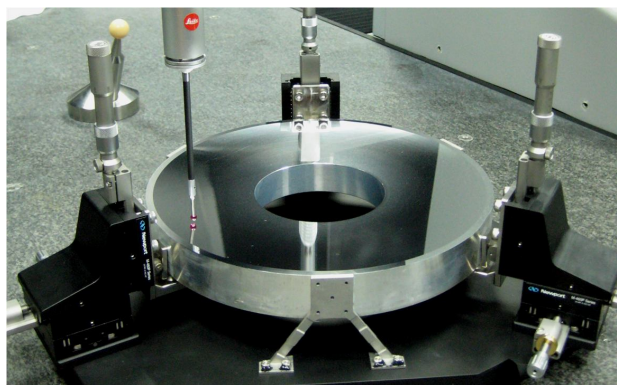


Figure 8. Primary mirror was bonded and aligned with main plate on auxiliary alignment fixture

After aligning, the primary mirror will be bonded with three ISMs by 3M DP490 structural adhesive and assembled with main plate. Three stages will be removed after adhesive curing.

4.2 Coordinate Measuring Machine Aided M1-M2 Alignment

Next process is coordinate measuring machine aided M1-M2 alignment, the M1-main plate assembly and M2 support ring assembly will be supported and assembled on the auxiliary assembling fixture. We used coordinate measuring machine to measure the surface of primary mirror and secondary mirror respectively, as shown in Figure 9. The calculated results from measured data provided the decenter, tilt and defocus magnitude of the secondary mirror

which is relative to primary mirror, then the orientation of the secondary mirror would be adjusted by adjustable supporting mechanism to eliminate the misalignment. After four rounds, the tilt and defocus of the M1-M2 optical system had been reduced to 13.9 arcsecond and $-3.3\mu\text{m}$, respectively.

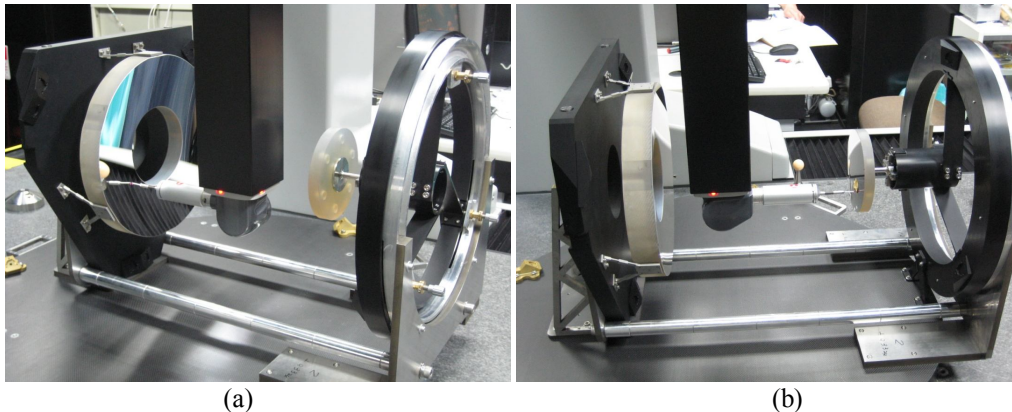


Figure 9. Experimental set up of coordinate measuring machine aided M1-M2 alignment. (a) Primary mirror surface measurement. (b) Secondary mirror surface measurement.

4.3 Interferometer Aided M1-M2 Alignment

After the coordinate measuring machine aided M1-M2 alignment process was accomplished, next step was interferometer aided M1-M2 alignment. In this process, the RSI ExM will be mounted on a trolley and the ESDI Intellium H1000 simultaneous interferometer, pinhole plate and 12 inch reference flat will be set up and aligned with RSI ExM, as shown in Figure 10. The ESDI Intellium H1000 simultaneous interferometer was mounted on a five axes stage. We operated the simultaneous interferometer to measure the wave front error (WFE) in five fields of the M1-M2 optical system, as shown in Figure 11. The measured fields were defined and constrained by the pinholes on pinhole plate which was aligned on the focal plane, as shown in the right of Figure 11(b). In order to estimate gravity effect and predict the optical system performance in zero gravity condition, we rotated the trolley upside down and measured the optical system in -1G condition, as shown in Figure 10(b).

In every measuring round, the result contains ten WFE data and these data will be transformed to Zernike polynomials, then are calculated and analyzed by optical design software Code V. Calculated results will provide the decenter, tilt and defocus magnitude of the secondary mirror for further adjustment and performance optimization.

After five alignment rounds, the decenter of the M1-M2 optical system had been reduced to $6.4\mu\text{m}$, and the minimum WFE_{rms} on optical axis was about 0.5λ . The performance of M1-M2 optical system had been optimized and the interferometer aided M1-M2 alignment process had been accomplished.

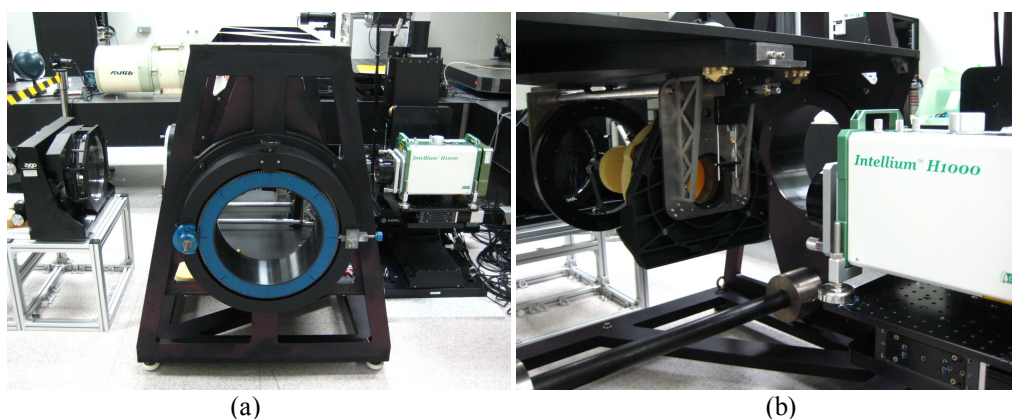


Figure 10. Experimental set up of interferometer aided M1-M2 alignment. (a) $+1\text{G}$ measurement. (b) -1G measurement.

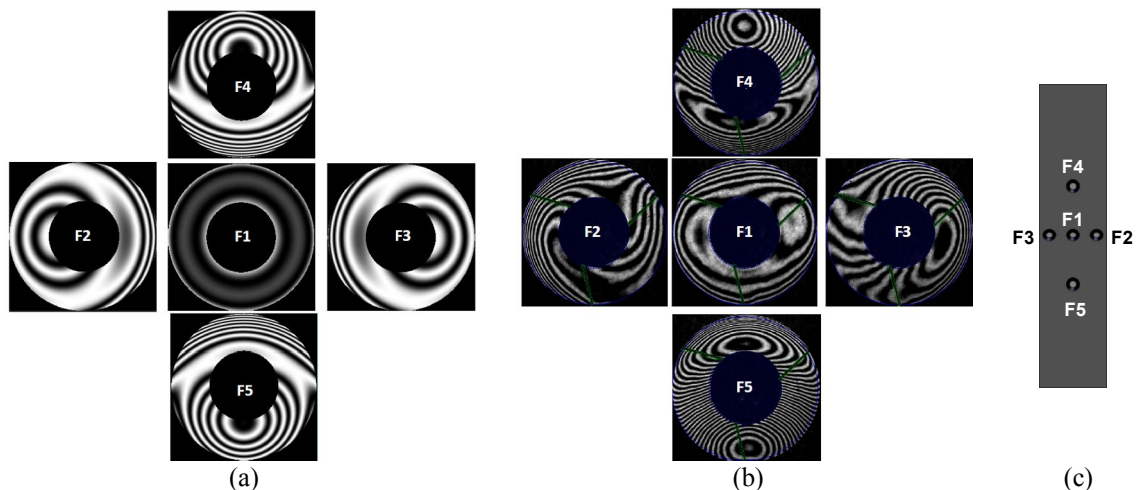


Figure 11. Interferograms of five fields. (a) Simulated interferograms of M1-M2 optical design. (b) Measured interferograms of 5th measuring round of M1-M2 optical system. (c) Pin hole allocations on pinhole plate

5. Conclusion

After interferometer aided M1-M2 alignment process, we will continue to implement the following alignment procedures, including truss structure assembly, interferometer aided corrector lens alignment, optical system performance measurement, focal plane assembly (FPA) and baffles alignment, system contrast transfer function (CTF) measurement and image test. The overall alignment processes of RSI ExM will be accomplished in the end of 2011.

In this project, RSI ExM really provides a very good platform to develop, implement and verify the telescope design, optical alignment technique and alignment procedure, from component level to system level. Many facilities, engineering techniques, analyses, methodologies and software have been developed and accomplished in this aerospace project. All of these techniques and experiences will provide good baseline for the following structure model (SM) and flight model (FM) of FORMOSAT-5 RSI.

Reference

- [1] Paul R. Yoder, Jr., 2006. Mounting Optics in Optical Instruments, third edition, SPIE press.
- [2] Paul R. Yoder, Jr., 2006. Opto-Mechanical Systems Design, third edition, SPIE press.
- [3] Robert E. Fischer, Biljana Tadic-Galeb, 2001. Optical System Design, McGraw-Hill.
- [4] Hookman, R., 1989. Design of the GOES telescope secondary mirror mounting. Proc. SPIE 1167, 368.
- [5] Meinel, A. and Meinel M., 1984. Zero-coma condition for decentered and tilted secondary mirror in Cassegrain/Nasmyth configuration. Opt. Eng., 23, 801.
- [6] Richard, R., 1990. Damping and vibration consideration for the design of optical systems in a launch/space environment. Proc. SPIE 1340, 82.
- [7] Barho, R., Stanghellini, S., and Jander, G., 1988. VLT secondary mirror unit performance and test results. Proc. SPIE 3352, 675.
- [8] Daniel Malacara., 2007. Optical Shop Testing. John Wiley & Sons.